PNAS RESEARCH ARTICLE | MICROBIOLOGY OPEN ACCESS

Interferon resistance of emerging SARS-CoV-2 variants

Kejun Guo[a], Bradley S. Barrett[a], James H. Morrison[a], Kaylee L. Mickens[a,b], Eszter K. Vladar[c], Kim J. Hasenkrug[d], Eric M. Poeschla[a,b,1], and Mario L. Santiago[a,b,1]

Edited by Jean-Laurent Casanova, The Rockefeller University, New York, NY; received March 3, 2022; accepted June 26, 2022

The emergence of SARS-CoV-2 variants with enhanced transmissibility, pathogenesis, and resistance to vaccines presents urgent challenges for curbing the COVID-19 pandemic. While Spike mutations that enhance virus infectivity or neutralizing antibody evasion may drive the emergence of these novel variants, studies documenting a critical role for interferon responses in the early control of SARS-CoV-2 infection, combined with the presence of viral genes that limit these responses, suggest that interferons may also influence SARS-CoV-2 evolution. Here, we compared the potency of 17 different human interferons against multiple viral lineages sampled during the course of the global outbreak, including ancestral and five major variants of concern that include the B.1.1.7 (alpha), B.1.351 (beta), P.1 (gamma), B.1.617.2 (delta), and B.1.1.529 (omicron) lineages. Our data reveal that relative to ancestral isolates, SARS-CoV-2 variants of concern exhibited increased interferon resistance, suggesting that evasion of innate immunity may be a significant, ongoing driving force for SARS-CoV-2 evolution. These findings have implications for the increased transmissibility and/or lethality of emerging variants and highlight the interferon subtypes that may be most successful in the treatment of early infections.

SARS-CoV-2 | COVID-19 | interferons | innate immunity | variants of concern

Significance

In just over 2 years, SARS-CoV-2 has infected 500 million people, causing more than 6 million COVID-19 deaths. High infection rates have provided substantial opportunities for the virus to evolve, as variants with enhanced transmissibility, pathogenesis, and resistance to neutralizing antibodies have emerged. While much focus has centered on the Spike protein, mutations were also detected in other viral proteins that may inhibit the interferons, two of which, IFNα2 and IFNβ, are being repurposed for COVID-19 treatment. Here, we compared the potency of diverse human interferons against ancestral and emerging variants of SARS-CoV-2. Our data revealed increased interferon resistance in SARS-CoV-2 variants of concern, suggesting a significant but underappreciated role for innate immunity in driving the next phase of the COVID-19 pandemic.

The human genome encodes a diverse array of antiviral interferons (IFNs). These include the type I IFNs (IFN-Is) such as the 12 IFNα subtypes IFNβ and IFNω that signal through the ubiquitous IFNAR (IFN α-receptor), and the type III IFNs (IFN-IIIs) such as IFNλ1, IFNλ2, and IFNλ3 that signal through the more restricted IFNλR receptor that is present in lung epithelial cells (1). IFN diversity may be driven by an evolutionary arms race in which viral pathogens and hosts reciprocally evolve countermeasures (2). For instance, the IFNα subtypes exhibit >78% amino acid sequence identity, but IFNα14, IFNα8, and IFNα6 most potently inhibited HIV-1 in vitro and in vivo (3–5), whereas IFNα5 most potently inhibited influenza H3N2 in lung explant cultures (6). Severe acute respiratory syndrome-coronavirus-2 (SARS-CoV-2) was sensitive to IFNα2, IFNβ, and IFNλ (7–9), and several clinical trials of IFNα2 and IFNβ demonstrated therapeutic promise for coronavirus disease 2019 (COVID-19) (10–12). A recent Phase III clinical trial demonstrating that IFNβ may not have therapeutic benefits in vivo (13) could be due to the late timing of administration among hospitalized/severely ill patients, cotreatment with glucocorticoids such as dexamethasone that directly antagonize IFN signaling (14), and the use of a subcutaneous route that may not efficiently target IFNs to pulmonary epithelial cells. To date, a direct comparison of multiple IFN-Is and IFN-IIIs against diverse SARS-CoV-2 variants of concern has not yet been done.

The present study was initiated to determine which IFNs would best inhibit SARS-CoV-2. Initially, we selected five isolates from prominent lineages (15) during the early phase of the pandemic (Fig. 1 and *SI Appendix*, Table S1). USA-WA1/2020 is the standard strain used in many in vitro and in vivo studies of SARS-CoV-2 and belongs to lineage A (15). It was isolated from the first COVID-19 patient in the United States, who had a direct epidemiologic link to Wuhan, China, where the virus was initially detected (16). By contrast, subsequent infection waves from Asia to Europe (17) were associated with the emergence of the D614G mutation (18). Lineage B strains with G614 spread globally and displaced ancestral viruses with striking speed, likely due to increased transmissibility (19, 20). These strains accumulated additional mutations in Italy as lineage B.1, which then precipitated a severe outbreak in New York City (21). Later, in the United Kingdom, lineage B.1.1.7 acquired an N501Y mutation associated with enhanced transmissibility (15). Lineage B.1.351, first reported in South Africa, additionally acquired an additional E484K mutation associated with resistance to neutralizing antibodies (22, 23). Both B.1.1.7 and B.1.351 were reported in multiple countries, and in some cases have become dominant for extended periods (24). Subsequent waves of infection after our initial preprint was deposited in March 2021 (25)

Author contributions: K.G., K.J.H., E.M.P., and M.L.S. designed research; K.G., B.S.B., K.L.M., E.K.V., J.H.M., E.M.P., and M.L.S. performed research; K.G., B.S.B., K.L.M., E.K.V., J.H.M., K.J.H., E.M.P., and M.L.S. contributed new reagents/analytic tools; K.G., B.S.B., K.L.M., E.K.V., J.H.M., K.J.H., E.M.P., and M.L.S. analyzed data; and K.G., B.S.B., E.K.V., J.H.M., K.J.H., E.M.P., and M.L.S. wrote the paper.

The authors declare no competing interest.

This article is a PNAS Direct Submission.

[1]To whom correspondence may be addressed: eric.poeschla@cuanschutz.edu, mario.santiago@cuanschutz.edu.

This article contains supporting information online at http://www.pnas.org/lookup/suppl/doi:10.1073/pnas.2203760119/-/DCSupplemental.

Published July 22, 2022.

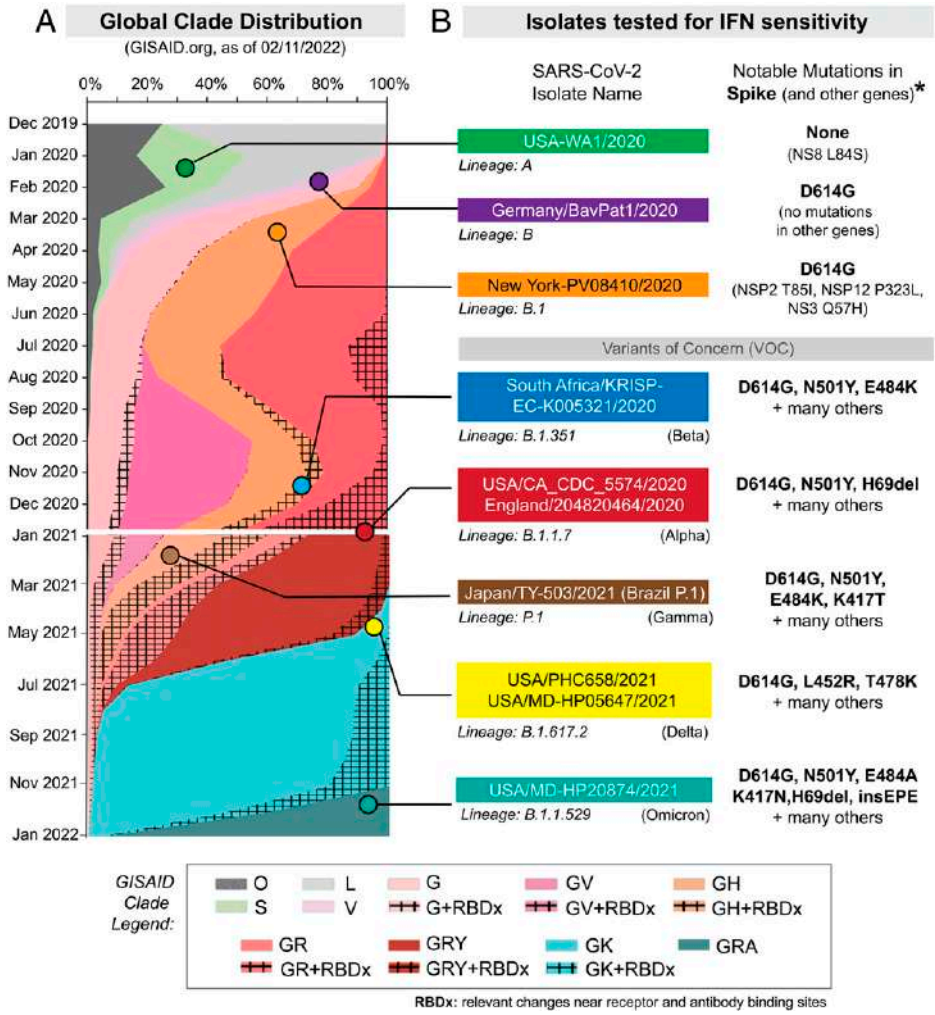

Fig. 1. Selection of SARS-CoV-2 strains for IFN sensitivity studies. (*A*) Global distribution of SARS-CoV-2 clades. GISAID.org plotted the proportion of deposited sequences in designated clades against collection dates. The 10 isolates chosen are noted by colored dots. (*B*) SARS-CoV-2 strains selected for this study included representatives of lineages A, B, B.1, B.1.351, and B.1.1.7 (*SI Appendix*, Table S1). Lineage P.1 (which branched off from lineage B.1.1.28), B.1.617.2, and B.1.1.529 were added after the initial preprint submission and were evaluated for IFNβ and IFNλ1 sensitivity. Lineage B isolates encode the D614G mutation associated with increased transmissibility. *Amino acid mutations were relative to the reference hCOV-19/Wuhan/WIV04/2019 sequence.

was associated with the P.1, B.1.617.2, and B.1.1.529 lineages (26–29). The emergence of these novel variants provided a unique opportunity to determine whether SARS-CoV-2 has evolved since its initial introduction into humans to better counteract innate immune selection pressures driven by the antiviral IFNs.

Results

Diverse IFNs Inhibited SARS-CoV-2 to Various Degrees In Vitro. During the first phase of this study from December 2020 to March 2021, we obtained representative SARS-CoV-2 isolates of the B, B.1, B.1.1.7, and B.1.351 lineages (Fig. 1 and *SI Appendix*, Table S1). Each stock was sourced from beiresources.org and amplified once in a human alveolar type II epithelial cell line (A549) that we have stably transduced with the receptor angiotensin-converting enzyme 2 (ACE2) (A549-ACE2) (*SI Appendix*, Fig. S1*A*). A549-ACE2 cells were preincubated with 17 recombinant IFNs (PBL Assay Science) overnight in parallel and in triplicate, then infected with a nonsaturating virus dose for 2 h (*SI Appendix*, Fig. S1*B*). We normalized the IFNs based on molar concentrations similarly to our previous work with HIV-1 (3, 30). To enable high-throughput evaluation of the antiviral activities of the numerous IFNs against the multiple live SARS-CoV-2 isolates, we used a quantitative PCR (qPCR) assay to determine the amounts of virus produced 24 h after infection (Fig. 2*A*). Initial dose titrations showed that a 2-pM concentration fell within the dynamic range of activity and maximally distinguished the antiviral activities of IFNs with widely divergent potencies (i.e., IFNβ and IFNλ1) (*SI Appendix*, Fig. S1*C*). The IFNβ and IFNλ1 doses used did not significantly affect cell viability (*SI Appendix*, Fig. S1*D*). Thus, 2 pM doses were used for additional antiviral activity testing. We also evaluated the qPCR assay against a VeroE6 plaque assay using triplicate serial dilutions of a SARS-CoV-2 isolate (B.1.351). Virus titers obtained using these two assays were strongly correlated (*SI Appendix*, Fig. S2*A*). However, the VeroE6 plaque assay had an ∼2-log lower dynamic range; we estimate that 1 plaque-forming unit corresponds to ∼900 SARS-CoV-2 N1 copies (*SI Appendix*, Fig. S2*A*). Virus copy numbers also correlated with the numbers of primary airway epithelial cells infected with different SARS-CoV-2 variants as quantified by immunofluorescence (*SI Appendix*, Fig. S2*B*). Thus, we used the qPCR assay to robustly distinguish the antiviral activity of the different IFNs.

In the absence of IFN, all five isolates reached titers of $\sim 10^4$–10^6 copies per 5 μL input of RNA extract (Fig. 2*A*). Using absolute copy numbers (Fig. 2*A*) or values normalized to mock as 100% (*SI Appendix*, Fig. S3), the 17 IFNs showed a

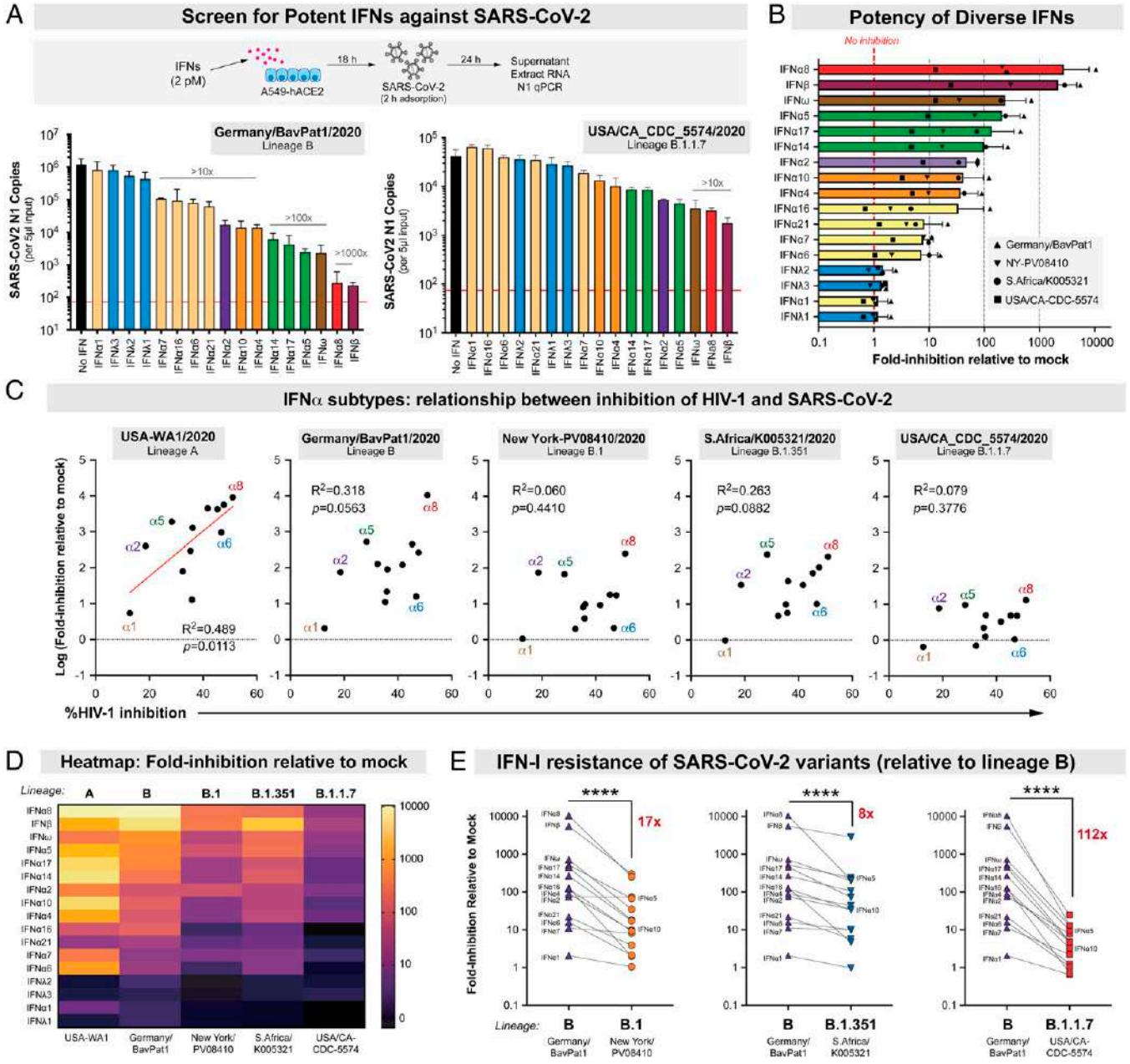

Fig. 2. Sensitivity of SARS-CoV-2 strains to IFN-I and IFN-III. (*A*) Antiviral assay using recombinant IFNs (2 pM) in A549-ACE2 cells. The red line corresponds to the qPCR detection limit (90 copies/reaction, or 1.8×10^4 copies/mL). Viral copy numbers in two D614G+ isolates, showing a similar rank order of IFNs from least to most potent. (*B*) The average fold inhibition relative to mock for lineage B, B.1, B.1.351, and B.1.1.7 isolates are shown. The most potent IFNs are shown top to bottom. Bars and error bars correspond to means and SDs. (*C*) Log-transformed IFN-inhibition values relative to mock for the five different SARS-CoV-2 strains were compared to previously published HIV-1 inhibition values, based on percentage of inhibition of HIV-1 $p24^+$ gut lymphocytes relative to mock as measured by flow cytometry (3). Each dot corresponds to an IFNα subtype. Linear regression was performed using GraphPad Prism. Significant correlations ($P < 0.05$) were highlighted with a red best-fit line. (*D*) Heatmap of fold inhibition of representative strains from the lineages noted. Colors were graded on a log-scale from highest inhibition (yellow) to no inhibition (black). (*E*) Comparison of IFN-I sensitivities between lineage B versus B.1, B.1.351, and B.1.1.7. The mean fold inhibition values relative to mock were compared in a pairwise fashion for the 14 IFN-Is. The average fold inhibition values were noted. Differences were evaluated using a nonparametric, two-tailed Wilcoxon matched-pairs signed rank test. NS, not significant; ****$P < 0.0001$.

range of antiviral activities against SARS-CoV-2. The 3 IFNλ subtypes exhibited none to very weak (less than twofold) antiviral activities compared to most IFN-Is (Fig. 2*A* and *SI Appendix*, Fig. S3, blue bars). The assay showed a robust dynamic range, with some IFNs inhibiting USA-WA1/2020 >2,500-fold to below detectable levels (*SI Appendix*, Fig. S3*A*). IFN potencies against the five isolates correlated with one another (*SI Appendix*, Fig. S4), and a similar rank order of IFN antiviral potency was observed for $G614^+$ isolates (Fig. 2*A* and *SI Appendix*, Fig. S3). Overall, IFNα8, IFNβ, and IFNω were the most potent, followed by IFNα5, IFNα17, and IFNα14 (Fig. 2*B*); the type III (λ) IFNs were the least potent. We confirmed this hierarchy by generating inhibition curves for five IFNs, showing that IFNλ1 had 100-fold higher half-maximal inhibitory concentration (IC_{50}) than IFNα2, which in turn exhibited 14-fold higher IC_{50} than IFNβ, IFNα5, and IFNα8 (*SI Appendix*, Fig. S5).

The molecular basis for the diverse antiviral effects of the highly related IFNα subtypes has been an active area of investigation, particularly in regard to the relative contributions of quantitative (signaling) versus qualitative (differential gene regulation) mechanisms (2–5). We reported that inhibition of

HIV-1 by the IFNα subtypes correlated with IFNAR signaling capacity and binding affinity to the IFNAR2 subunit (3, 30). IFNAR signaling capacity, as measured in an IFN-sensitive reporter cell line (iLite cells; Euro Diagnostics), correlated with the antiviral potencies of the IFNα subtypes against ancestral SARS-CoV-2 lineages A and B, but not lineages B.1, B.1.351, or B.1.1.7 (*SI Appendix*, Fig. S6*A*). IFNAR binding affinities as measured by surface plasmon resonance by the Lavoie group (31) did not correlate with IFNα subtype inhibition of SARS-CoV-2 (*SI Appendix*, Fig. S6*B*). As the recombinant IFNs used in this study were from the same source as that of the prior HIV-1 study (3, 30), we also determined whether the IFNs that potently inhibit HIV-1 also function similarly against SARS-CoV-2. Notably, IFNα subtype inhibition of HIV-1 (3) did not significantly correlate with IFNα subtype inhibition of the majority of the SARS-CoV-2 isolates we tested (Fig. 2*C*). These findings suggested that IFN-mediated control of SARS-CoV-2 isolates may be qualitatively distinct from that of HIV-1.

Emerging SARS-CoV-2 Variants Were More Resistant to Antiviral IFNs than Ancestral Isolates. We generated a heatmap to visualize the antiviral potency of diverse IFNs against the five isolates and observed marked differences in IFN sensitivities (Fig. 2*D*). Pairwise analysis of antiviral potencies between isolates collected early (January 2020) and later (March–December 2020) during the pandemic were performed against the 14 IFN-Is (IFN-III data were not included due to low antiviral activity; Fig. 2*B* and *SI Appendix*, Fig. S3). The overall IFN-I sensitivity of USA-WA1/2020 and Germany/BavPat1/2020 isolates were not significantly different from one another (*SI Appendix*, Fig. S7*A*). In contrast, relative to Germany/BavPat1/2020, we observed 17- to 122-fold IFN-I resistance of the emerging SARS-CoV-2 variants (Fig. 2*E*), with the B.1.1.7 strain exhibiting the highest IFN-I resistance (this can also be seen in Fig. 2*D*). The level of IFN resistance was especially striking when compared to the early pandemic USA-WA1/2020 strain, in which emerging SARS-CoV-2 variants exhibited 25- to 322-fold higher IFN-I resistance (*SI Appendix*, Fig. S7*B*).

The experiments to this point allowed for the simultaneous analysis of 17 IFNs against multiple SARS-CoV-2 isolates, but did not provide information as to how different IFN-I doses affect the replication of distinct virus strains. It also remained unclear whether the emerging variants were resistant to IFN-IIIs. We therefore titrated a potent (IFNβ; 0.002–200 pM) and a weak (IFNλ1; 0.02–2,000 pM) IFN against the lineage A, B, B.1, B.1.1.7, and B.1.351 viruses (Fig. 3*A* and *B* and *SI Appendix*, Fig. S7*C* and *D*). Of note, IFNβ and IFNλ1 were also detected in COVID-19 patients (32, 33). IFN titrations against each emerging variant included the lineage B isolate (Germany/BavPat1/2020) as an internal control. Importantly, as the pandemic progressed after March 2021, new variants of concern (VOCs) became dominant in several countries; the World Health Organization implemented a simplified Greek letter nomenclature for these VOCs. We therefore included five additional VOC isolates, which were also obtained from the Biodefense and Emerging Infections (BEI) repository: (1) a second B.1.1.7 (Alpha) isolate, England/204820464/2020; (2) an isolate from lineage P.1 (Gamma), which branched off from lineage B.1.1.28; (3) two isolates from lineage B.1.617.2 (Delta) that encoded an intact or defective ORF7a, a viral protein that may be involved in IFN antagonism (34, 35); and (4) an isolate from the most dominant variant as of this writing, B.1.1.529 (Omicron) (*SI Appendix*, Table S1). Lineage P.1, an offshoot of the B.1.1.28 lineage, was first described in an outbreak of SARS-CoV-2 in Manaus, Brazil, which occurred in a population with high levels of prior infection (26). P.1 independently acquired the E484K mutation (Fig. 1*A* and *SI Appendix*, Table S1). The Delta strain was first reported in India in early 2021, and became the dominant variant worldwide from July 2021, including the United States (Fig. 1). The Delta strain was frequently observed in breakthrough infections among fully vaccinated individuals (27). Following its initial detection in southern African countries, the Omicron variant became the dominant strain worldwide by late December 2021, with peak infection levels more than four times higher than that of Delta (28). Omicron was distinguished by the unprecedentedly high levels of mutations in Spike, which enabled it to efficiently evade natural and vaccine-elicited humoral immunity (36).

The lineage A and B isolates were similarly inhibited by IFNβ and IFNλ1 (Fig. 3*A*; see also *SI Appendix*, Fig. S7*A*). Comparing B to B.1, the IC_{50} of the B.1 isolate was 2.6- and 5.5-fold higher IC_{50} for IFNλ1 and IFNβ, respectively (*SI Appendix*, Fig. S7*C*). Relative to lineage B, the Alpha variant IC_{50}s were 4.3- to 8.3-fold higher for IFNβ and 3.0- to 3.5-fold higher for IFNλ1 (Fig. 3*B*). Interestingly, maximum inhibition was not achieved with either IFNβ or IFNλ1 against the alpha VOCs, plateauing at 15- to 20-fold higher levels than the ancestral lineage B isolate (Fig. 3*B*), which was in sharp contrast to the lineage B.1 isolate (*SI Appendix*, Fig. S7*C*). In a separate experiment, the Beta isolate was also more resistant to IFNβ (5-fold) and IFNλ1 (21-fold) compared to the lineage B isolate (Fig. 3*C*). Here, however, maximum inhibition was achieved with IFNβ. The Gamma variant exhibited higher resistance to IFNβ (1.9-fold) and IFNλ1 (4.4-fold), and the plateau concentration for antiviral activity was >10-fold higher for IFNβ than for the lineage B isolate (Fig. 3*D*). The two Delta isolates tested were more resistant to IFNβ (6.7- and 3.2-fold) than lineage B. Interestingly, the $ORF7a^-$ Delta isolate had 2.1-fold higher IC_{50} than the $ORF7a^+$ isolate (Fig. 3E). Finally, the Omicron variant had 5.9- and 6.6-fold higher IC_{50} than the lineage B isolate for IFNβ and IFNλ1, respectively (Fig. 3*F*). The plateau at the highest IFN doses was 178-fold higher for IFNβ and 13-fold higher for IFNλ1 than the lineage B isolates (Fig. 3*F*). Overall, the five VOCs exhibited 5.1-fold and 4.4-fold higher IC_{50} for IFNβ and IFNλ1, respectively, relative to the ancestral lineage B isolate (Fig. 3*G*). Moreover, the VOCs showed 9.2-fold higher levels of residual replication at the highest IFNλ1 doses (Fig. 3*H*). Residual virus titers were not significantly higher for VOCs at the highest IFNβ dose tested, but this value was disproportionately high for the Omicron variant relative to the other VOCs (Fig. 3*H*).

Two months after our initial preprint (25), Thorne et al. posted data that in Calu-3 cells, an Alpha isolate was more resistant to IFNβ than a "first wave" lineage B isolate (37). We found that lineage A and B isolates replicated poorly in Calu-3 cells, making these cells unsuitable for IFN resistance comparisons between ancestral versus emerging variants (*SI Appendix*, Fig. S8*A*). This was in sharp contrast to A549-ACE2 cells, in which we observed high levels of virus production (at least 10^5 copies) of all of the strains studied (Fig. 2*A* and *SI Appendix*, Fig. S3). Notably, comparable titers were obtained between the B.1 and Alpha isolates in Calu-3 cells (*SI Appendix*, Fig. S8*B*). In these cells, the Alpha isolate was 50-fold more resistant to IFNλ1 than the B.1 isolate (*SI Appendix*, Fig. S8*B*). We also demonstrate that the Alpha and Delta isolates were more resistant to IFNβ than the B.1 isolate in Calu-3 cells (*SI Appendix*, Fig. S8*C*).

Evidence for Increasing IFN Resistance of SARS-CoV-2 in Primary Human Bronchial Epithelial Cells (HBECs). A549-ACE2 and Calu-3 cells allowed for robust comparisons of the potency of

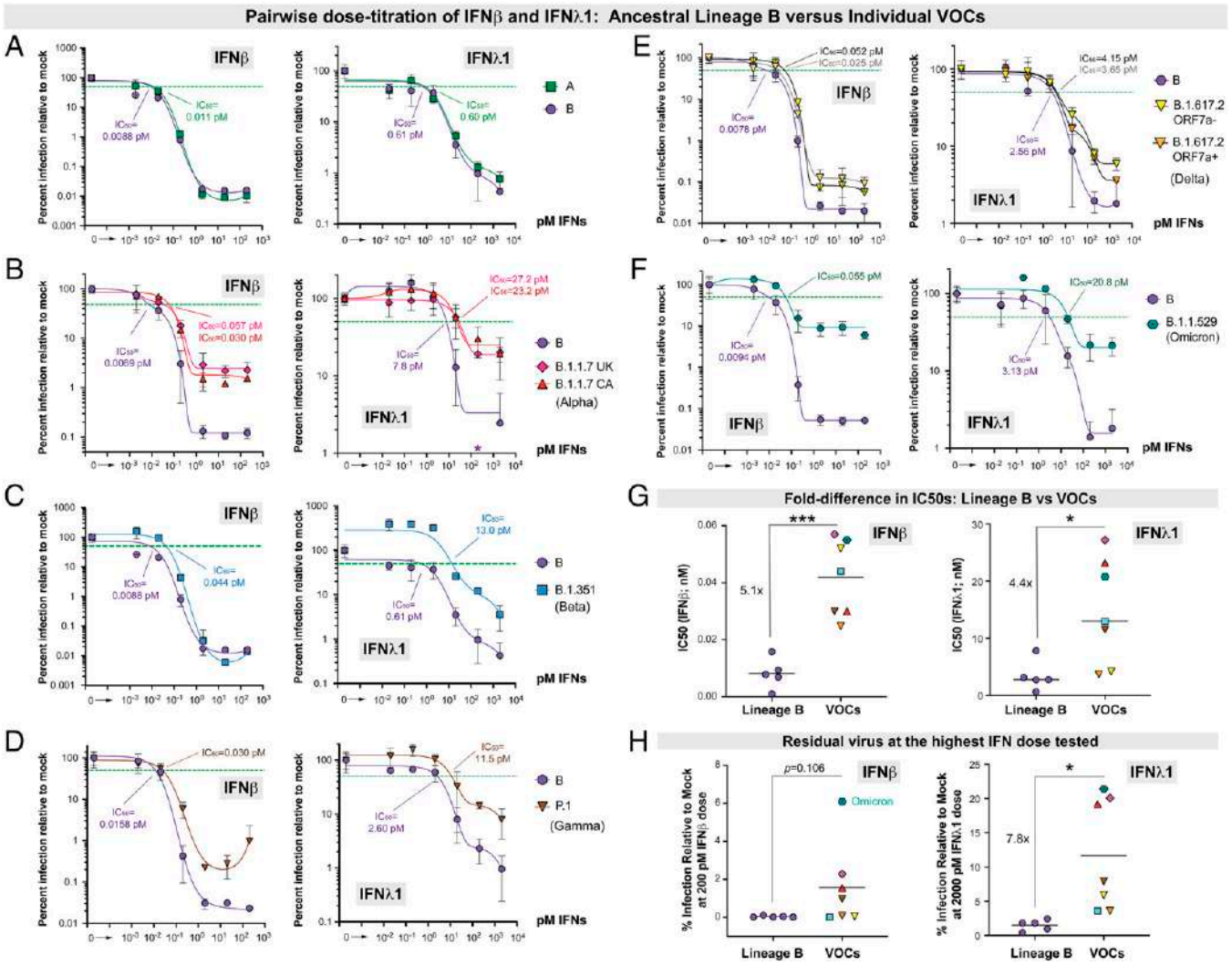

Fig. 3. Dose titration of ancestral lineage B versus five variants of concern against IFNβ and IFNλ1. IFNβ and IFNλ1 dose titrations in (*A*)–(*F*) correspond to separate infections and used the lineage B isolate Germany/BavPat1/2020 isolate as a control. A549-ACE2 cells were pretreated with serial 10-fold dilutions of IFNs for 18 h in triplicate and then infected with SARS-CoV-2. Supernatants were collected after 24 h, SARS-CoV-2 N1 copy numbers were determined by qPCR in triplicate, and then the mean copy numbers were normalized against mock as 100%. Error bars correspond to SDs. Nonlinear best-fit regression curves of mean normalized infection levels were used to interpolate IC_{50}s (green dotted lines). IFN sensitivity of the ancestral lineage B isolate was compared to (*A*) ancestral lineage A (USA-WA1/2020); (*B*) B.1.1.7 (Alpha) isolates USA/CA_CDC_5574/2020 (CA) and England/204820464/2020 (UK); (*C*) B.1.351 (Beta) (South Africa/KRISP-EC-K005321/2020); (*D*) P.1 (Gamma) (Japan/TY7-503/2021); (*E*) B.1.617.2 (Delta) isolates USA/PHC658/2021 (ORF7a$^-$) and USA/MD-HP05647/2021 (ORF7a$^+$); and (*F*) B.1.1.529 (Omicron) (USA/MD-HP20874/2021). *In (*B*), the datapoint at 200 pM IFNλ1 for lineage B (0.54) precluded efforts for IC_{50} determination and was excluded in the curve fitting. In (*A*) and (*C*), the datapoint for lineage B at 0.002 pM IFNβ was excluded as the inhibition curve was significantly skewed to the left relative to four other lineage B titrations. (*F*) IC_{50} and (*G*) residual infection levels at the highest IFN doses were compared between lineage B (five independent titrations) and VOCs. Datapoint shapes and colors correspond to those in (*A*)–(*F*). Differences in the mean values were evaluated using a two-tailed Student's *t* test or Mann-Whitney *U* test, depending on whether the data distribution was normal. *$P < 0.05$; ***$P < 0.001$. Fold differences between lineage B and VOCs are indicated.

multiple IFNs against diverse SARS-CoV-2 isolates. However, these cell lines may not completely recapitulate the biology of primary lung epithelial cells. Therefore, we used air–liquid interface (ALI) cultures of primary HBECs (Fig. 4*A*) (39). HBEC cultures challenged with lineage A, lineage B, and 3 major VOCs Alpha, Delta, and Omicron were tracked for up to 4 d in the presence or absence of IFNβ (Fig. 4B) at 2 pM, a dose within the dynamic range of inhibition for all strains (*SI Appendix*, Fig. S1 and Figs. 2*D* and 3*A*–*E*). Most isolates grew to high titers except for lineage B, which replicated approximately 1–2 logs lower (*SI Appendix*, Fig. S9*A*, *Upper Panel*). Normalization to mock conditions for each isolate at 4 dpi suggested differences in the levels of inhibition (ANOVA, $P < 0.05$; *SI Appendix*, Fig. S9*A*, *Lower panel*), with the Omicron isolate being the most resistant to IFNβ. When plotted against the date when the virus was identified, we observed a significant increase in IFNβ resistance with time (Fig. 4*C*, *Left Panel*). To determine whether these apply to other IFNs, we performed a similar experiment on HBECs with IFNα2 and IFNλ1, which, like IFNβ, are being tested in human clinical trials as potential therapies against COVID-19. Normalizing to mock conditions for each isolate (*SI Appendix*, Fig. S9*B* and *C*), we again observed a similar increase in IFNα2 and IFNλ1 resistance with time (Fig. 4*C*, *Middle* and *Right Panels*). These findings suggest that SARS-CoV-2 is evolving to resist diverse antiviral IFNs during the course of the COVID-19 pandemic.

Discussion

Numerous studies have shown that IFNs are important for host defense against SARS-CoV-2. This sarbecovirus is believed to have recently crossed the species barrier to humans, either directly from bats or via an intermediate mammalian host(s) (40). Here,

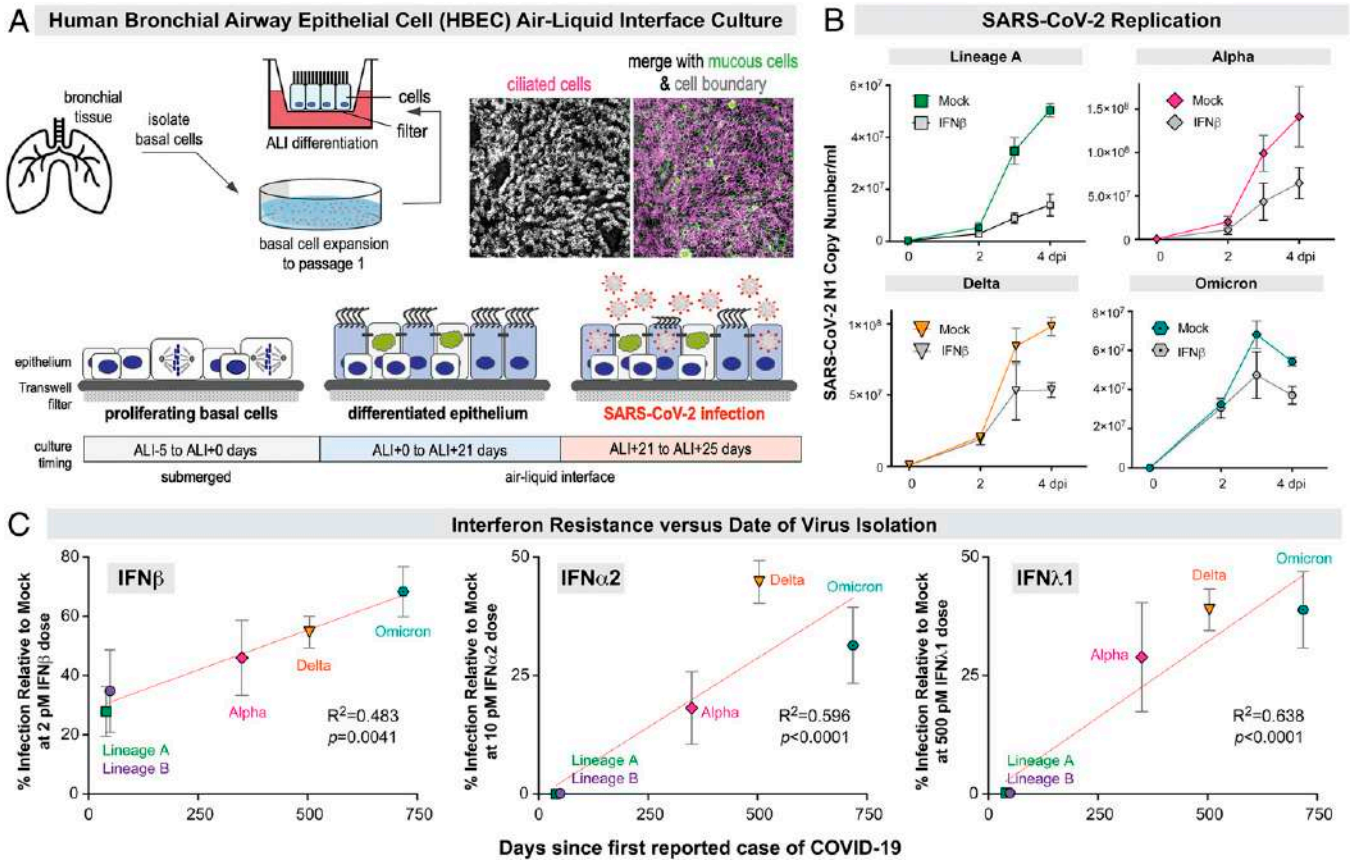

Fig. 4. Evidence for increasing IFN resistance of SARS-CoV-2 in primary HBECs during the course of the COVID-19 pandemic. (*A*) Basal stem cells from healthy donor airway tissue were used to generate HBEC cultures. (*Upper Left*) Basal cells were isolated from human donor lungs, expanded to passage 1, and then differentiated at ALI on Transwell filters. (*Upper Right*) En face view of whole-mount-labeled ALI at day 21 (ALI+21d). Mature HBECs contain a large number of ciliated (red) and mucous (green) cells. (*Lower Panel*) Schematic of ALI culture and SARS-CoV-2 infection timeline. At ALI+21d, untreated or IFN-treated HBECs were infected in quadruplicate with 10^8 vRNA N1 copies of SARS-CoV-2 strains representing lineage A (USA-WA1/2020), lineage B (Germany/BavPat1/2020), Alpha (England/204820464/2020), Delta (USA/MD/HP05647/2021), and Omicron (USA/MD-HP20874/2021). (*B*) Apical viral shedding up to 4 dpi was determined by qPCR quantification of viral N1 RNA copies. Mean copy numbers per microliter input are shown ±SEMs for 2 h and 2, 3, and 4 dpi, showing that differences between mock- and IFNβ-treated cells became more apparent at 4 dpi. (*C*) Relative sensitivity of globally dominant SARS-CoV-2 isolates in HBECs against (*Left*) IFNβ, (*Center*) IFNα2, and (*Right*) IFNλ1, plotted with time since the first COVID-19 case reported on December 10, 2019 (day 0) (38). Error bars correspond to SEMs in quadruplicate experiments. Correlations were evaluated by linear regression.

we demonstrate that SARS-CoV-2 has in fact evolved after host switching to become more resistant to human IFNs. Moreover, we establish an order of antiviral potency for the diverse type I and III IFNs. IFNλ initially showed promise as an antiviral that can reduce inflammation (41), but our data suggest that for SARS-CoV-2, higher doses of IFNλ may be needed to achieve a similar antiviral effect in vivo as the IFN-Is. Nebulized IFNβ showed potential as a therapeutic against COVID-19 (11), and our data confirm that IFNβ is highly potent against SARS-CoV-2. However, IFNβ was also linked to pathogenic outcomes in chronic mucosal HIV-1 (30), murine lymphocytic choriomeningitis virus (42) and, if administered late in mice, SARS-CoV-1 and Middle East respiratory syndrome-CoV (43, 44) infection. We previously reported that IFNβ up-regulated 2.4-fold more genes than individual IFNα subtypes, suggesting that IFNβ may induce more pleiotropic effects (30). Among the IFNα subtypes, IFNα8 showed an anti-SARS-CoV-2 potency similar to that of IFNβ. IFNα8 also exhibited high antiviral activity against HIV-1 (3), raising its potential for treatment against both pandemic viruses. Notably, IFNα8 appeared to be an outlier in this regard, as the antiviral potencies of the IFNα subtypes against SARS-CoV-2 and HIV-1 did not correlate strongly. IFNα6 potently restricted HIV-1 (3, 4) but was one of the weakest IFNα subtypes against SARS-CoV-2. Conversely, IFNα5 strongly inhibited SARS-CoV-2, but weakly inhibited HIV-1 (3). This lack of correlation is a key point for future studies. Of note, the high potency of IFNα5 and low potency of IFNα6 against an isolate of SARS-CoV-2 (not a VOC) were corroborated by another group (45). Collectively, these data strengthen the theory that diverse IFNs may have evolved to restrict distinct virus families (2, 30). The mechanisms underlying these interesting qualitative differences remain unclear. While IFNAR signaling contributes to antiviral potency (3, 4, 31), diverse IFNs may have distinct abilities to mobilize antiviral effectors in specific cell types. Comparing the interferomes induced by distinct IFNs in lung epithelial cells (45) may be useful in prioritizing further studies on this point.

Most significantly, our data reveal the concerning trend for SARS-CoV-2 variants emerging later in the pandemic—in the setting of prolific replication of the virus in human populations—to resist the antiviral IFN response. Before the present work, the emergence and fixation of variants was linked to enhanced viral infectivity and/or neutralizing antibody evasion due to mutations in the Spike protein. However, previous studies with HIV-1 suggested that IFNs also can shape the evolution of pandemic viruses (46, 47). In fact, SARS-CoV-2-infected individuals with either genetic defects in IFN signaling (48) or IFN-reactive autoantibodies (49) had an increased risk of developing severe COVID-19. As IFNs are critical in controlling early virus infection levels, IFN-resistant SARS-CoV-2 variants may produce higher viral loads that could in turn promote transmission

and/or exacerbate pathogenesis. Consistent with this hypothesis, the alpha VOC was associated with increased viral loads (50) and risk of death (51). Infection with Delta may yield even higher viral loads than that with Alpha (52), but to date, no discernible differences in viral loads were found between Delta and Omicron (53). Notably, our data on IFN resistance partially tracked with consecutive waves of the most dominant global VOCs Alpha, Delta, and Omicron. Alpha, as well as the Beta and Gamma VOCs that circulated concurrently, was more IFN resistant than ancestral isolates. Delta was more sensitive or had similar IFN sensitivity compared to Alpha in A549-ACE2 and Calu-3 cells, respectively. This suggested that other factors, such as increased transmissibility and resistance to neutralizing antibodies, may have contributed to the shift from Alpha to Delta. Notably, the most infectious variant to date, Omicron, had the highest levels of residual virus replication at the highest doses of IFNβ, one of the most potent IFNs we determined in this study. Alpha and Delta replicate efficiently in the lower respiratory tract; by contrast, Omicron appeared to replicate predominantly in the upper respiratory tract (53), which was proposed to be the main site of protective IFN action in vivo (32). Primary human bronchial airway epithelial cells are physiologically relevant models of the upper airway epithelial compartment (39). In these cells, Delta and Omicron were more resistant to IFNβ, IFNα2, and IFNλ1 than Alpha. In fact, our data in primary HBEC cultures suggested that SARS-CoV-2 resistance to IFNs may be increasing during the course of the COVID-19 pandemic.

In addition to Spike, emerging variants exhibit mutations in nucleocapsid, membrane, and nonstructural proteins NSP3, NSP6, and NSP12 (*SI Appendix*, Table S1). In the case of early pandemic viruses that predated the emergence of VOCs, these viral proteins were reported to antagonize IFN signaling in cells (36, 54). To specifically map the virus mutations driving IFN-I resistance in emerging variants, panels of recombinant viruses can be generated to isolate specific mutations, singly or in combination against various IFNs, and candidate single viral protein antagonists can be individually tested as well. This would help to confirm, for example, that the D3L mutation in the Alpha nucleocapsid may facilitate innate immune evasion by increasing the expression of an IFN antagonist, ORF9b (37). Of note, the nucleocapsid D3L mutation was not observed in the Beta, Gamma, Delta, and Omicron lineages (*SI Appendix*, Table S1), which exhibited IFN-I and IFN-III resistance in our experiments. One of the Delta isolates we studied had a deletion in ORF7a, which may counteract IFN signaling (34, 35); this deletion was not a cell culture artifact as it was also observed in the clinical isolate. We tested another Delta isolate with an intact ORF7a and it exhibited similar, or even higher, IFN sensitivity. This would suggest that ORF7a may not be a dominant mechanism contributing to IFN antagonism in live virus. In *SI Appendix*, Table S2, we highlight mutations in nucleocapsid, NSP12, and NSP6 in multiple VOCs, which may confer IFN resistance and will be prioritized in subsequent work. It is possible that mutations in multiple viral proteins may synergize to confer IFN resistance and that the combinatorial effect of these mutations may differ between the various VOCs.

Overall, the present study suggested a role for the innate immune response in driving the evolution of SARS-CoV-2 that could have practical implications for IFN-based therapies. Our findings reinforce the importance of continued full-genome surveillance of SARS-CoV-2, and assessments of emerging variants not only for resistance to vaccine-elicited neutralizing antibodies, but also for evasion of the host IFN response.

Materials and Methods

Virus Isolates. SARS-CoV-2 stocks were obtained from BEI Resources (www.beiresources.org). *SI Appendix*, Table S1 provides detailed information on the source of the material, the catalog, and lot numbers and virus sequence information of both the clinical and cultured stocks. See *SI Appendix, Materials and Methods* for further details.

SARS-CoV-2 qPCR. Total RNA was extracted from 100 μL culture supernatant using the E.Z.N.A. Total RNA Kit I (Omega Bio-Tek) and eluted in 50 μL RNase-free water. Five microliters of this extract were used in a one-step reverse transcriptase-quantitative PCR reaction (New England Biolabs) using official Centers for Disease Control and Prevention (CDC) SARS-CoV-2 nucleocapsid (N1) gene primers and probe. The real-time qPCR reaction was run on a Bio-Rad CFX96 real-time thermocycler. See *SI Appendix, Materials and Methods* for further details.

Antiviral Inhibition Assay. Recombinant IFNs were obtained from PBL Assay Science. Amplified virus stock yielding ~10^5 copies per 5 μL input RNA extract was used for the IFN inhibition assay (*SI Appendix*, Fig. S1*B*). Initially, we tested 17 IFNs using a 2-pM dose (Fig. S1*C*). Subsequently, 50% inhibitory concentrations were determined using 10-fold serial dilutions of IFNβ and IFNλ1. Infections were performed in 48-well plates seeded with 2.5×10^4 A549-ACE2 cells preincubated for 18 h with the IFNs. Cells were infected with virus for 2 h, washed twice with phosphate-buffered saline, and then 500 μL complete media was added. The cultures were incubated for another 24 h, after which, supernatants were harvested for RNA extraction and qPCR analysis. See *SI Appendix, Materials and Methods* for further details.

Data Availability. All of the study data are included in the article and/or supporting information.

ACKNOWLEDGMENTS. We thank Cara Wilson, Magdalena Sotelo, Ulf Dittmer, and Kathrin Gibbert for scientific advice; Mercedes Rincon and Elan Eisenmesser for assistance with the construction and characterization of the A549-ACE2 cells; Zach Wilson, Jill Garvey, Stephanie Torres-Nemeti, Brett Haltiwanger, and Marcia Finucane for Biosafety Level 3 infrastructure support; and Roman Wölfel, Rosina Ehmann, Adolfo García-Sastre, Alex Sigal, Tulio de Oliveira, Bassam Hallis, Matsuyo Takayama-Ito, Richard Webby, Anami Patel, Andrew Pekosz, Cathleen Seager, BEI Resources (National Institute of Allergy and Infectious Diseases), and the CDC for the SARS-CoV-2 isolates.

This work was supported by the Division of Infectious Diseases, Department of Medicine, University of Colorado (M.L.S.); the Tietze Foundation (E.M.P.), the National Institutes of Health R01 AI134220 (M.L.S.); the Cystic Fibrosis Foundation COVID-19 Research Grant 00169G220 (E.K.V.); and the Intramural Research Program at the National Institute of Allergy and Infectious Diseases, National Institutes of Health (K.J.H.). The funders had no role in study design, data collection and analysis, decision to publish, or preparation of the manuscript.

Author affiliations: [a]Division of Infectious Diseases, Department of Medicine, University of Colorado Anschutz Medical Campus, Aurora, CO 80045; [b]Department of Immunology and Microbiology, University of Colorado Anschutz Medical Campus, Aurora, CO 80045; [c]Division of Pulmonary Sciences and Critical Care Medicine, Department of Medicine, University of Colorado Anschutz Medical Campus, Aurora, CO 80045; and [d]Rocky Mountain Laboratories, National Institutes of Allergy and Infectious Diseases, National Institutes of Health, Hamilton, MT 59840

1. S. Pestka, C. D. Krause, M. R. Walter, Interferons, interferon-like cytokines, and their receptors. *Immunol. Rev.* **202**, 8–32 (2004).
2. K. Gibbert, J. F. Schlaak, D. Yang, U. Dittmer, IFN-α subtypes: Distinct biological activities in antiviral therapy. *Br. J. Pharmacol.* **168**, 1048–1058 (2013).
3. M. S. Harper *et al.*, Interferon-α subtypes in an ex vivo model of acute HIV-1 infection: Expression, potency and effector mechanisms. *PLoS Pathog.* **11**, e1005254 (2015).
4. E. Schlaepfer *et al.*, Dose-dependent differences in HIV inhibition by different interferon alpha subtypes while having overall similar biologic effects. *MSphere* **4**, e00637-18 (2019).

5. K. J. Lavender *et al.*, Interferon alpha subtype-specific suppression of HIV-1 infection in vivo. *J. Virol.* **90**, 6001–6013 (2016).
6. A. D. R. Matos *et al.*, Antiviral potential of human IFN-α subtypes against influenza A H3N2 infection in human lung explants reveals subtype-specific activities. *Emerg. Microbes Infect.* **8**, 1763–1776 (2019).
7. A. Vanderheiden *et al.*, Type I and type III interferons restrict SARS-CoV-2 infection of human airway epithelial cultures. *J. Virol.* **94**, e00985-20 (2020).
8. U. Felgenhauer *et al.*, Inhibition of SARS-CoV-2 by type I and type III interferons. *J. Biol. Chem.* **295**, 13958–13964 (2020).
9. R. Nchioua *et al.*, SARS-CoV-2 is restricted by zinc finger antiviral protein despite preadaptation to the low-CpG environment in humans. *MBio* **11**, e01930-20 (2020).
10. N. Wang *et al.*, Retrospective multicenter cohort study shows early interferon therapy is associated with favorable clinical responses in COVID-19 patients. *Cell Host Microbe* **28**, 455–464.e2 (2020).
11. P. D. Monk *et al.*, Safety and efficacy of inhaled nebulised interferon beta-1a (SNG001) for treatment of SARS-CoV-2 infection: A randomised, double-blind, placebo-controlled, phase 2 trial. *Lancet Respir. Med.* **9**, 196–206 (2020).
12. S. Shalhoub, Interferon beta-1b for COVID-19. *Lancet* **395**, 1670–1671 (2020).
13. A. C. Kalil *et al.*; ACTT-3 Study Group Members, Efficacy of interferon beta-1a plus remdesivir compared with remdesivir alone in hospitalised adults with COVID-19: A double-bind, randomised, placebo-controlled, phase 3 trial. *Lancet Respir. Med.* **9**, 1365–1376 (2021).
14. S. Gessani, S. McCandless, C. Baglioni, The glucocorticoid dexamethasone inhibits synthesis of interferon by decreasing the level of its mRNA. *J. Biol. Chem.* **263**, 7454–7457 (1988).
15. A. Rambaut *et al.*, A dynamic nomenclature proposal for SARS-CoV-2 lineages to assist genomic epidemiology. *Nat. Microbiol.* **5**, 1403–1407 (2020).
16. P. Zhou *et al.*, A pneumonia outbreak associated with a new coronavirus of probable bat origin. *Nature* **579**, 270–273 (2020).
17. M. Worobey *et al.*, The emergence of SARS-CoV-2 in Europe and North America. *Science* **370**, 564–570 (2020).
18. B. Korber *et al.*; Sheffield COVID-19 Genomics Group, Tracking changes in SARS-CoV-2 spike: Evidence that D614G increases infectivity of the COVID-19 virus. *Cell* **182**, 812–827.e19 (2020).
19. J. A. Plante *et al.*, Spike mutation D614G alters SARS-CoV-2 fitness. *Nature* **592**, 116–121 (2021).
20. Y. J. Hou *et al.*, SARS-CoV-2 D614G variant exhibits efficient replication ex vivo and transmission in vivo. *Science* **370**, 1464–1468 (2020).
21. A. S. Gonzalez-Reiche *et al.*, Introductions and early spread of SARS-CoV-2 in the New York City area. *Science* **369**, 297–301 (2020).
22. C. K. Wibmer *et al.*, SARS-CoV-2 501Y.V2 escapes neutralization by South African COVID-19 donor plasma. *Nat. Med.* **27**, 622–625 (2021).
23. P. Wang *et al.*, Antibody resistance of SARS-CoV-2 variants B.1.351 and B.1.1.7. *Nature* **593**, 130–135 (2021).
24. S. E. Galloway *et al.*, Emergence of SARS-CoV-2 B.1.1.7 Lineage - United States, December 29, 2020-January 12, 2021. *MMWR Morb. Mortal. Wkly. Rep.* **70**, 95–99 (2021).
25. K. Guo *et al.*, Interferon resistance of emerging SARS-CoV-2 variants. *bioRxiv* [Preprint] (2021). 10.1101/2021.03.20.436257 (Accessed 21 March 2021).
26. N. R. Faria *et al.*, Genomics and epidemiology of the P.1 SARS-CoV-2 lineage in Manaus, Brazil. *Science* **372**, 815–821 (2021).
27. C. M. Brown *et al.*, Outbreak of SARS-CoV-2 infections, including COVID-19 vaccine breakthrough infections, associated with large public gatherings–Barnstable County, Massachusetts, July 2021. *MMWR Morb. Mortal. Wkly. Rep.* **70**, 1059–1062 (2021).
28. The New York Times, Coronavirus in the U.S.: Latest map and case count (2021). https://www.nytimes.com/interactive/2021/world/covid-cases.html. Accessed 2 March 2022.
29. K. Tao *et al.*, The biological and clinical significance of emerging SARS-CoV-2 variants. *Nat. Rev. Genet.* **22**, 757–773 (2021).
30. K. Guo *et al.*, Qualitative differences between the IFNα subtypes and IFNβ influence chronic mucosal HIV-1 pathogenesis. *PLoS Pathog.* **16**, e1008986 (2020).
31. T. B. Lavoie *et al.*, Binding and activity of all human alpha interferon subtypes. *Cytokine* **56**, 282–289 (2011).
32. B. Sposito *et al.*, The interferon landscape along the respiratory tract impacts the severity of COVID-19. *Cell* **184**, 4953–4968.e16 (2021).
33. M. D. Galbraith *et al.*, Specialized interferon action in COVID-19. *Proc. Natl. Acad. Sci. U.S.A.* **119**, e2116730119 (2022).
34. L. Martin-Sancho *et al.*, Functional landscape of SARS-CoV-2 cellular restriction. *Mol. Cell* **81**, 2656–2668.e8 (2021).
35. H. Xia *et al.*, Evasion of type I interferon by SARS-CoV-2. *Cell Rep.* **33**, 108234 (2020).
36. D. Planas *et al.*, Considerable escape of SARS-CoV-2 Omicron to antibody neutralization. *Nature* **602**, 671–675 (2022).
37. L. G. Thorne *et al.*, Evolution of enhanced innate immune evasion by the SARS-CoV-2 B.1.1.7 UK variant. *bioRxiv* [Preprint] (2021). 10.1101/2021.06.06.446826 (Accessed 7 June 2021).
38. M. Worobey, Dissecting the early COVID-19 cases in Wuhan. *Science* **374**, 1202–1204 (2021).
39. E. K. Vladar, J. V. Nayak, C. E. Milla, J. D. Axelrod, Airway epithelial homeostasis and planar cell polarity signaling depend on multiciliated cell differentiation. *JCI Insight* **1**, e88027 (2016).
40. E. C. Holmes *et al.*, The origins of SARS-CoV-2: A critical review. *Cell* **184**, 4848–4856 (2021).
41. S. Davidson *et al.*, IFNλ is a potent anti-influenza therapeutic without the inflammatory side effects of IFNα treatment. *EMBO Mol. Med.* **8**, 1099–1112 (2016).
42. C. T. Ng *et al.*, Blockade of interferon beta, but not interferon alpha, signaling controls persistent viral infection. *Cell Host Microbe* **17**, 653–661 (2015).
43. R. Channappanavar *et al.*, IFN-I response timing relative to virus replication determines MERS coronavirus infection outcomes. *J. Clin. Invest.* **129**, 3625–3639 (2019).
44. R. Channappanavar *et al.*, Dysregulated type I interferon and inflammatory monocyte-macrophage responses cause lethal pneumonia in SARS-CoV-infected mice. *Cell Host Microbe* **19**, 181–193 (2016).
45. J. Schuhenn *et al.*, Differential interferon-α subtype induced immune signatures are associated with suppression of SARS-CoV-2 infection. *Proc. Natl. Acad. Sci. U.S.A.* **119**, e2111600119 (2022).
46. S. S. Iyer *et al.*, Resistance to type 1 interferons is a major determinant of HIV-1 transmission fitness. *Proc. Natl. Acad. Sci. U.S.A.* **114**, E590–E599 (2017).
47. M. V. P. Gondim *et al.*, Heightened resistance to host type 1 interferons characterizes HIV-1 at transmission and after antiretroviral therapy interruption. *Sci. Transl. Med.* **13**, eabd8179 (2021).
48. Q. Zhang *et al.*; COVID-STORM Clinicians; COVID Clinicians; Imagine COVID Group; French COVID Cohort Study Group; CoV-Contact Cohort; Amsterdam UMC Covid-19 Biobank; COVID Human Genetic Effort; NIAID-USUHS/TAGC COVID Immunity Group, Inborn errors of type I IFN immunity in patients with life-threatening COVID-19. *Science* **370**, eabd4570 (2020).
49. P. Bastard *et al.*; HGID Lab; NIAID-USUHS Immune Response to COVID Group; COVID Clinicians; COVID-STORM Clinicians; Imagine COVID Group; French COVID Cohort Study Group; Milieu Intérieur Consortium; CoV-Contact Cohort; Amsterdam UMC Covid-19 Biobank; COVID Human Genetic Effort, Autoantibodies against type I IFNs in patients with life-threatening COVID-19. *Science* **370**, eabd4585 (2020).
50. M. Kidd *et al.*, S-variant SARS-CoV-2 lineage B1.1.7 is associated with significantly higher viral loads in samples tested by ThermoFisher TaqPath RT-qPCR. *J. Inf. Dis.* **223**, 1666–1670 (2021).
51. N. G. Davies *et al.*; CMMID COVID-19 Working Group, Increased mortality in community-tested cases of SARS-CoV-2 lineage B.1.1.7. *Nature* **593**, 270–274 (2021).
52. S. W. X. Ong *et al.*, Clinical and virological features of SARS-CoV-2 variants of concern: A retrospective cohort study comparing B.1.1.7 (Alpha), B.1.315 (Beta), and B.1.617.2 (Delta). *Clin. Infect. Dis.* ciab721, DOI: 10.1093/cid/ciab721. (2021).
53. M. Kozlov, Omicron's feeble attack on the lungs could make it less dangerous. *Nature* **601**, 177 (2022).
54. X. Lei *et al.*, Activation and evasion of type I interferon responses by SARS-CoV-2. *Nat. Commun.* **11**, 3810 (2020).